N94-11395

The Efficiency of Photovoltaic Cells Exposed to Pulsed Laser Light

R. A. Lowe, Cleveland State University, and G. A. Landis,
P. Jenkins, Sverdrup Technology, Inc.

Future space missions may use laser power beaming systems with a free electron laser (FEL) to transmit light to a photovoltaic array receiver. To investigate the efficiency of solar cells with pulsed laser light, several types of GaAs, Si, $CuInSe_2$, and GaSb cells were tested with the simulated pulse format of the induction and radio frequency (RF) FEL. The induction pulse format was simulated with an 800-watt average power copper vapor laser and the RF format with a frequency-doubled mode-locked Nd:YAG laser. Averaged current vs bias voltage measurements for each cell were taken at various optical power levels and the efficiency measured at the maximum power point.

Experimental results show that the conversion efficiency for the cells tested is highly dependent on cell minority carrier lifetime, the width and frequency of the pulses, load impedance, and the average incident power. Three main effects were found to decrease the efficiency of solar cells exposed to simulated FEL illumination: cell series resistance, LC "ringing", and output inductance. Improvements in efficiency were achieved by modifying the frequency response of the cell to match the spectral energy content of the laser pulse with external passive components.

Introduction

It is possible to send power over long distances by using a laser beam to transmit power to a receiving photovoltaic array [1,2]. Many potential space applications for beamed power systems have been identified. For example, satellites operating in Geosynchronous Earth orbit (GEO) are currently powered by solar arrays. Half of the mass of a satellite power system consists of batteries and other components performing regulating and charging functions of the batteries, with the sole function of providing power for less than 1% of the time. Laser light beamed from the ground could provide power during the eclipse period and reduce the mass of the satellite by eliminating or reducing the need for energy storage, or could be used to supplement solar power for satellites with degraded solar arrays [2]. For a photovoltaic-power system for a lunar base, power storage capability is required to supply power during the 354-hr. lunar night. A laser used to illuminate an array during the night would substantially reduce the storage mass [3,4]. For an orbital transfer vehicle, electric rocket engines (ion engines, plasmadynamic thrusters) have high specific impulse but require large amounts of power. For a vehicle configured with such engines the amount of fuel required could be reduced with a beamed power/PV array system. Such a vehicle would provide an efficient LEO to GEO or LEO to lunar orbit shuttle [5].

A beamed power system would consist of one or more ground-based lasers, an adaptive optics system to compensate for atmospheric distortion, a large optical element at each laser site to shape and direct the beam, and photovoltaic (PV) arrays as receivers [2]. Several types of lasers have been investigated for space power transmission. The free-electron laser (FEL) is especially

attractive because of its potentially high efficiency, tunability over a wide wavelength range, and potential for high average power operation [6]. Lasers used for power beaming must operate in the portion of the visible or NIR spectrum which efficiently penetrates the atmosphere. While a RF-FEL has demonstrated operation at wavelengths as short as 550 nm [7], a FEL has not yet been demonstrated combining both the high average power required for power beaming and the short wavelength operation required for Si and GaAs solar cells.

Previous studies have investigated the efficiency of solar cells with continuous-wave lasers [1,8,9]. However, FEL lasers are by nature pulsed. Pulsed operation of photovoltaic cells at high average power has significant differences from operation under continuous illumination [10]. Until this work, operation of cells in this regime has not been tested.

There are two main designs of free-electron laser, differing in the type of accelerator used to produce the electron beam: the induction FEL and the the radio-frequency FEL. The pulse formats produced by the two accelerator types are significantly different.

The induction FEL will have characteristically 10-50 nanosecond wide pulses at maximum repetition frequencies on the order of ten kilohertz. The induction FEL considered for power beaming [11] will produce pulses 50 nS wide, seperated by 100 μS (10 kHz), producing a duty factor of 1:2000. This is a somewhat optimistic projection of future improvements in efficiency for induction accelerators.

A RF FEL, on the other hand, will produce pulses with a width of 5-10 picoseconds (referred to as "micropulses"), at a repetition rate of tens of megahertz. In some designs of RF FEL, the series of RF micropulses will then be repetitively pulsed, for a "macropulse".

The proposed RF FEL for quasi-CW operation (i.e., a continuous string of micropulses), has a pulse width of 15 to 20 pS, with 27 nS between pulses (repetition rate 36 MHz, the 12th harmonic of the RF frequency of 433 MHz). This gives a duty factor for the micropulse of about 1:1500 [12]. An alternative variation is a pulsed laser. A pulsed RF FEL may be more efficient to operate at lower power levels. The RF FEL [13] also modulates the micropulses with a 5 μS macropulse at a 1 kHz repetition rate, for a macropulse duty factor of 1:200.

Near the maximum power bias point of a solar cell, the output from the cell is expected to stretch the input pulse by an amount comparable to the minority-carrier lifetime of the semiconductor (more properly, by a weighted average of the emitter and base minority-carrier lifetimes). The response to pulsed illumination will thus depend on whether the spacing between pulses is significantly greater than, or significantly less than, the minority carrier lifetime in the semiconductor [8]. For direct bandgap materials such as GaAs, the minority carrier lifetimes are typically on the order of nanoseconds [14]. Since the spacing between pulses for the induction laser is significantly larger than the lifetime, it is expected that the output of the GaAs cells will not significantly stretch the pulse, and hence the cells will respond to the peak incident power. For indirect bandgap materials such as Si, the minority carrier lifetimes are typically on the order of microseconds [15]. Since this is on the order of the spacing between pulses for the induction laser, it is expected that the output from silicon cells will significantly stretch the pulse, and hence the cell will tend to average the pulses.

For the RF FEL, the minority carrier lifetime is comparable or longer than the spacing between micropulses for all the materials, and hence the output pulse from the solar cell is expected to be stretched nearly to CW. However, the spacing between macropulses (for the pulsed RF FEL) is significantly longer than the minority carrier lifetime for either GaAs or Si, and hence the cell output should follow the macropulse.

In an effort to understand the issues involved in using PV cells to convert power transmitted by a free electron laser, a study was undertaken to measure the efficiency of a wide variety of PV cells

with rapidly pulsed lasers. The main purpose of this experiment was to test the response of cells to the induction FEL pulse format, however, for comparison, several of the cells were also tested using a laser which simulated the pulsed RF FEL pulses.

Cells Tested

Several different types of cell, made from four different semiconductor materials, were tested. Table 1 lists the types of cells tested. Silicon, an indirect bandgap material, has long minority carrier lifetime. GaAs, GaSb, and $CuInSe_2$ were tested as examples of direct bandgap, and hence short minority carrier lifetime, materials.

Before testing, the cells efficiencies and current-voltage (I-V) characteristics were measured under the simulated air-mass zero (AM0) spectrum (25°C, 137 mW/cm^2), the dark diode characteristics were measured, and the cell internal series resistances were calculated by comparison of the dark diode characteristic with the V_{oc}-I_{sc} characteristic using the method of Rajkanan [16]. Representative cells were also measured for capacitance at zero bias.

Silicon cells: Silicon (Si) cells are used for primary power for almost all satellites currently in orbit. Several types of silicon cells were measured. Cells typical of satellites currently in orbit were studied, including a cell with radiation damage of 5×10^{14} electrons/cm^2, typical of the conditions encountered after ~20 years in geosynchronous orbit. In addition, several cells of more advanced design were measured, including concentrator cell types designed for high peak currents. The highest efficiency Si cell tested was a low resistivity (0.15 Ω-cm base) cell manufactured using the high-efficiency, low resistance laser-grooved process [17].

GaAs cells. Gallium arsenide (GaAs) cells have higher efficiency than silicon cells, and will be used for missions where high efficiency is critical. Cells from several manufacturers were tested. Two general configurations were measured: flat-panel cells and concentrator cells. The flat-panel cells are typical of existing satellite solar array designs, but are poorly designed for the high peak current output expected for the peak of the laser pulse. The concentrator cell designs [15,16] are small area cells with low series resistance, and are designed to have much better response to high peak currents.

GaSb cells. Gallium antimonide (GaSb) cells are not currently used on satellites; however, for some applications, it has been suggested that it may be desirable to use an "eyesafe" laser wavelength greater than 1400 nm, a wavelength range to which neither silicon nor GaAs cells will respond. GaSb cells were tested as typical of cell types which may operate in this wavelength regime.

$CuInSe_2$ cells. Copper indium diselenide ($CuInSe_2$) cells are also not currently used on satellites. Such cells currently have much lower efficiencies than silicon or GaAs cells and are not made in versions acceptable for space operation, however, it has been suggested that future thin-film arrays may use $CuInSe_2$ cells.

In addition to the tests of the solar cells alone, one GaAs cell was also tested with capacitors of 500 nF and 4.4 μF added directly to the cell to smooth the peak current transients and thus reduce inductive effects.

Laser Systems

The laser wavelengths used for the test were 521±11 nm. Three laser systems were employed to simulate the FEL pulse formats. Efficiency under CW laser illumination was measured using an Argon-ion laser operating at a wavelength of 514.5 nm, at an intensity of 165 mW/cm^2.

The induction FEL pulse format was simulated using a 800-watt average power copper vapor laser (CVL) with associated optics to provide beam attenuation and uniformity. The pulse width, shown in fig. 1a, is 38 ns (FWHM) with a PRF (pulse repetition frequency) of 8.6 Khz. The 572 nm component of the CVL light was dichroically separated from the beam, leaving the 511 nm collimated beam incident on the PV cells.

Finally, for some of the cells, the pulse format of a pulsed RF FEL was simulated with a frequency doubled mode-locked Nd:YAG laser operating at 532 nm. The micropulse structure consisted of a 100 picosecond FWHM pulse with a spacing of 10 ns. These micropulses were modulated by an approximately rectangular macropulse with a duration of 4 μs and a PRF of 10 Hz. The laser pulse format is shown in fig. 1b. While a 100 pS micropulse is considerably longer than the 15 pS pulses expected from a RF FEL operating at 840 nm, both the 100 pS pulses simulated and the 15 pS expected are both significantly less than the minority carrier lifetimes, and hence little difference is expected.

The laser wavelengths were chosen for the availability of high-power lasers with the pulse format required. For power beaming operation, however, it is expected that the laser wavelength will be chosen at a value near the wavelength of peak monochromatic efficiency of the solar cell. This wavelength is in the range of 840 nm for typical GaAs cells, 950-1000 nm for silicon cells (without radiation damage), and about 1600 nm for GaSb cells. Radiation damage will shift the monochromatic efficiency peak to shorter wavelengths.

Efficiencies measured at the test wavelength l must be corrected to the desired operating wavelength. This is done by a wavelength correction factor

$$\frac{\text{Efficiency at } \lambda(1)}{\text{Efficiency at } \lambda(2)} = \frac{\lambda(1)}{\lambda(2)}[QE(\lambda(1))/QE(\lambda(2))] \qquad (1)$$

The wavelength term accounts for the fact that for constant photon flux, the incident power is inversely proportional to the wavelength. The quantum efficiency term accounts for the fact that the probability of collection of an electron-hole pair created by absorption of a photon will have some dependence on the depth of penetration of the light, and hence the wavelength. For the high-efficiency cells tested, the quantum efficiency (QE(l)) is not strongly dependent on the wavelength at the wavelengths of interest below the band edge. To within the measurement accuracy, the correction factor may be estimated as equal to the ratio of the wavelengths (except for the radiation-damaged silicon cell, where the long-wavelength quantum efficiency is preferentially damaged.)

The correction factors shown in table 2 are used to translate data from the test wavelength to the desired operating wavelength. The efficiency is multiplied by the correction factor. The effective laser power must be divided by the correction factor, thus keeping the photon flux constant.

Use of this correction factor implicitly assumes that the time dependence of the output response of the solar cell is independent of the wavelength of the incident light. This is not strictly correct. Short wavelength light is absorbed near the junction, and the generated electron-hole pairs are collected quickly. Since longer wavelength light is absorbed deeper in the material, however, the response to the long wavelength light will be slightly slower. This will result in a slightly different output waveform for the response to light near the band edge of the material due to the additional time for carriers to be collected by the junction. However, the amount by which the output pulse can be stretched is at most equal to the minority carrier lifetime in the cell base. This is small enough that the difference will not alter the main conclusions of the experiment.

Measurement Apparatus

The experimental apparatus is shown in fig. 2. The apparatus was designed to measure both the average power output of the cell, which is important to operation of a power system, and also to measure the instantaneous current and voltage as a function of time. The cell is mounted on an electrically isolated stage with a large heatsink and a thermocouple to measure cell temperature. Temperature did not rise significantly during the test.

A 11,000 μfd capacitor mounted near the cell integrates the AC current pulse generated by the cell. The average DC output current through the load is measured with a DC milliammeter. The lead length and parasitic inductance between the cell and capacitor is minimized to reduce the induced voltage generated by the large current transient during the pulse. A minimum wire length of 3 cm was required for the current pick-up; additional wiring in the system added 2-3 cm. A digital sampling oscilloscope with a 200 Mhz inductive current pickup and a 3.5 Ghz high-impedance sampling head were utilized to obtain the current and voltage waveforms out of the cell, and 16 to 128 waveforms were averaged to reduce noise.

The conversion efficiency value for the inductive FEL is calculated from the bias applied to the cell (V_{bias}), the average current delivered by the cell (I_{out}), and the energy incident on the cell using

$$\eta = \frac{P_{out}}{P_{in} A} \tag{2}$$

where $P_{out} = I_{out} \times V_{bias}$ is the electrical power output of the cell at the maximum power point, P_{in} is the radiant energy input in mW/cm^2, and A is the area of the cell in cm^2. The cell bias voltage was varied to find the maximum power point. I_{out} and V_{bias} here are DC values. This is thus the average efficiency over the laser cycle, including both the illuminated and dark periods of the cycle. While the instantaneous efficiency during one particular instant of the pulse may be higher, this DC efficiency is a good measure of power obtainable in an operational situation. As a check, these efficiency values were verified by comparison with the power dissipated by use of a purely resistive load.

A bias voltage was provided with a variable bipolar power supply, allowing various points on the cell operating I-V curve to be measured. For pulsed operation, there is a significant difference in efficiency that depends on whether a resistive or a constant voltage bias is used. The source used provided an approximation to a constant-voltage bias; this is typical of a satellite power bus. While a constant voltage bias provides a better match to the maximum power point of the cell during intensity variation, the cell dark current adds a constant power loss during both the illuminated and the dark portion of the pulse. Use of a blocking diode can nearly eliminate this dark current loss, at the cost of the diode voltage drop.

For the RF FEL simulation, a slightly different data acquisition system was used to allow measurements at the low pulse repetition rate. Voltage and current waveform acquisition over the macropulse were made with a 400 Mhz digitizing sampling oscilloscope.

Efficiency measured for the RF FEL was done by averaging the energy output during a macropulse, divided by the incident energy measured with a radiometer. The cell bias voltage was varied to find the maximum power point. This was then averaged over 32 pulses to reduce the noise. Again, $P_{out} = I_{avg} \times V_{bias}$; however, for this measurement I_{avg} was measured from the output current waveform measured by the oscilloscope, rather than from an independent ammeter.

As a comparison, the measured current V(t) and voltage I(t) were multiplied to find the time dependent output power P(t) which was integrated to find the total energy:

$$P_{out} = \int_0^{t_o} v(t)i(t)dt \qquad (3)$$

where t_o is the duration of the pulse.

Results

Table 3 shows the efficiency of PV cells tested under CW laser illumination, compared with pulsed laser illumination with the induction laser format. The power listed is the average power. For the inductive format the pulse duty cycle (at FWHM) is approximately 1:3200. The maximum power in the pulse is 3200 times the average power. Measurements were made at an incident average power level of 253 mW/cm^2 (1.85 suns, where one sun intensity is 137 mW/cm^2), and then at reduced intensities of 25 and 2.5 mW/cm^2 (0.185 and 0.019 suns respectively). These intensities correspond to peak powers of 5920, 592, and 59 suns. Table 4 shows the wavelength corrected efficiencies of Si, GaAs, and GaSb cells using the correction factors from table 2 for the induction FEL.

Three cells were also tested using the RF laser format. The efficiency calculated by the current times the bias was compared with efficiency based on the total energy produced from the time-dependant power curve, equation (3). This data is shown in table 5. For the RF FEL, the power is the average power delivered over the duration of one macropulse (4 μs). The cells tested with the RF FEL format are exposed to a lower average power. Since the PRF of the Nd:YAG laser was very

low, 10Hz, the duty cycle of the laser is only 1:25000. The laser power for this test was set to simulate the same peak power as an RF-FEL with a repetitive (macro) pulse rate of 1 kHz. The average power delivered during the 4 μS macropulse was thus about 16.7 W/cm^2 (122 suns).

As discussed, the average efficiency measured with the RF laser simulation included only the efficiency during the macropulse. If the efficiency over the entire pulse string is to be considered, the power loss due to dark reverse current between macropulses must be subtracted from the power. Table 6 shows the DC bias voltage at maximum power and the measured dark reverse current at the bias voltage for the GaAs and Si cells for both lasers.

Discussion:

Illumination of the solar cells with the induction FEL pulse format resulted in significant decreases in efficiency of the solar cells measured, compared to the continuous-wave laser. At all except the lowest intensities, the silicon cells outperformed the GaAs cells. This is as expected from the longer minority carrier lifetimes.

Three main effects decrease the efficiency of the solar cells for the induction-FEL format pulsed illumination:

1. Series Resistance. For the laser format used, the peak power during the pulse (8.6 kHz, 38 nS FWHM) is 3200 times the average power. Thus, for short lifetime cells, the peak output current must be 3200 times the average current for the cell to respond. I^2R losses due to the series resistance of the cell reduce the performance severely.

For example, the lowest resistance cell measured had a series resistance designed for operation at 850 times solar concentration, well below the 3200x in the experiment. In addition, the series resistance limits the peak current to

$I < V_{OC}/R$

2. L-C "Ringing." A solar cell is essentially a large-area p-n junction, and thus has a large junction capacitance. This, in conjunction with the necessary inductance of the output wiring, results in LC oscillations. Such oscillations result in operation of the cell at a bias different from the peak power point, and hence reduce the power.

3. Output inductance. The inductance L of the output wiring results in a maximum rate of increase in current:

$dI/dt \leq V_{OC}/L$

and hence, the cell is held at open-circuit voltage for a time

$t \approx (LI_{SC})/V_{OC}$

during which it produces little power.

Note that this experiment used wire lengths on the order of 3 cm, far shorter (and hence, far lower inductance) than would be found in any real-life solar array. These effects are discussed below.

At the highest intensity level, 5600 suns peak (approx. 2 suns avg.), of the induction-format pulse, the efficiency is the lowest for each cell. This is due to series-resistance limiting of internal cell

voltage by high current. Fig. 3 shows the effect of series resistance limiting on Si, GaAs, $CuInSe_2$, and GaSb cells at 5600 suns peak (253 mW/cm^2). At the next lower intensity, 560 suns peak, the efficiency of all cells improve. The effect on the peak output current is minimal with a 10x reduction in the input power causing the efficiency to increase significantly. At 56 suns peak intensity the efficiency for the Si cells has leveled off or dropped slightly, with the exception of the radiation-damaged cell, where the minority carrier lifetime has been degraded and the series resistance increased. The efficiency is improved at the lowest intensity because of the high series resistance of 1.9 ohms.

An LRC circuit is formed by the junction capacitance of the cell and the parasitic resistance and inductance in the leads and capacitors. Where insufficient resistance is present for damping a characteristic "ringing" is present in the voltage and current. For a purely resistive load attached to the cell the power delivered depends on

$$p(t) = \frac{1}{T}\int_0^T v(t)i(t)dt \tag{5}$$

where V(t) and I(t) are periodic signals with period T. Reactive elements in the circuit cause a difference in phase angle between the output current and voltage. The power delivered to a resistive load is proportional to cos(f), where f is the phase angle difference between V(t) and I(t). Resistance in the circuit decreases the phase angle but causes a loss in efficiency by forcing cell output voltage to V_{OC}. Phase angle may also be reduced by limiting inductance in the circuit. This approach is impractical because at very high frequencies the induced voltages generated by parasitic inductance in short leads, capacitors, and resistors are unavoidable.

An integrating capacitor across the cell converts the AC pulsed output to DC, a form more suitable for distribution. The energy delivered to the capacitor from the cell is a function of voltage and is independent of phase angle. Energy losses in a capacitive load are confined to leakage current, parasitic resistance, and dielectric loss. Additional circuit losses are the cell dark diode current and, similar for a resistive load, resistive dissipation within the cell-circuit during oscillation. A significant improvement in efficiency for cells with oscillating transients can be achieved by mounting a small capacitor (100 nF-500 nF) across the cell contacts. The small capacitor reduces the effect of the induced EMF when the cell discharges current into the inductance of the integrating capacitor leads. As a result, a larger portion of the energy is transferred to the integrating capacitor and less energy is dissipated in the cell. For example, the output voltage and current of the VS 850x GaAs concentrator cell at 253 mW/cm^2 is shown in fig. 4a,b. Fig. 4c,d is the output voltage and current with a 500 nF capacitor across the cell terminals. The efficiency with a 500 nF capacitor was measured at 4.5 % as compared to 2.0 % for the uncompensated cell. The improvement in cell efficiency with the addition of passive devices will be addressed more completely in a future paper.

Induced voltage caused by the interaction of large current transients with the parasitic inductance in the cell interconnects and series resistance losses in the cell are the major causes of efficiency loss. Voltage developed across the cell during the onset of the laser pulse is due to the electric field generated by charged carrier separation and the induced voltage

$$V_i = L\frac{dI}{dt} \tag{4}$$

where V_i is the induced voltage, L is the parasitic inductance in the cell leads, and dI/dt is the time rate of change of the current waveform. Fig. 5 shows the current and voltage response of a 2x2 cm GaAs cell to a CVL (induction FEL format) pulse at I_{sc}. The initial slope of the current waveform with ΔI = .88 A and Δt = 40 ns is $2.2x10^7$ amps/sec. Using an estimate of L = 35 nH for the cell lead/integrating cap. inductance, V_i is 770 mv. This is the significant factor forcing the cell output to V_{oc} in the first 20 ns. During the next 100 ns cell output voltage is held at V_{oc} and large amounts of current are dissipated in the cell contributing to a loss in efficiency. Minimizing this effect using short leads and high frequency capacitors is possible, however, even short leads (3 cm) possess enough parasitic inductance to produce prohibitively large induced voltages.

Minority carrier lifetime affects the falltime of the cell output current and voltage. Fig. 6 shows the current and voltage response of a long lifetime Si cell such as the ASEC 10 ohm cm. The time for the voltage to decay to 10 % of its maximum value differs by a factor of 13 (8 ms for Si vs .6 ms for GaAs in fig. 4). As minority carrier lifetime increases carriers diffuse to the depletion region for a longer duration of time and are collected as current. A high carrier mobility will tend to offset this effect in a short minority carrier lifetime material such as GaAs.

Cell voltage bias affects the shape of the output waveform by reducing ringing. The load, consisting of a voltage supply that can sink current, presents a constantly varying impedance $\hat{Z}_{load} = V_{bias}/\hat{I}_{cell}$ to the cell. Figure 7 a,b show the voltage output waveform of a GaAs concentrator cell biased at 0V and .520V (P_{max}) respectively. At P_{max} the impedance is larger due to increased V_{bias}, reduced $\hat{I}_{cell}$, and the cell output oscillations are damped. For other cells, fig. 7 c,d, damping was evident but the effect was not as pronounced. Reducing oscillation and eliminating the phase angle difference between $\hat{V}_{cell}$ and $\hat{I}_{cell}$ increases the power delivered to a resistive load and improves the efficiency of the cell.

Conclusion

Experimental results show the conversion efficiency of photovoltaic cells to pulsed laser light, for existing cell designs tested, is highly dependent on the cell minority carrier lifetime, the width and frequency of the pulses, and average incident power. Factors such as matching source wavelength to the bandgap energy of the PV material and minimizing series resistance are critical in designing efficient PV cells for a laser power beaming system. For cells with short minority carrier lifetimes, resistance and high-frequency electrical effects caused by short laser pulses prohibit efficient operation of the cell and transfer of power to a load. Future cell designs for a pulsed laser system would need to address the AC response of the cell and interconnects and reducing series resistance for efficient operation at high power levels. Modification of the cell's AC response utilizing external passive components may also prove effective in improving efficiency.

Acknowledgements: Peter Iles, ASEC; Mark Spitzer, Kopin; VS, Boeing, Herbert Friedman, Livermore; Rocketdyne, Bruce Anspaugh and Bob Mueller; NASA JPL

References

1. C.E. Backus, Conf. Record 9th IEEE Photovoltaic Specialists Conf., Silver Spring, MD, May 1972, 61-65.

2. G. A. Landis, 26th Intersociety Energy Conversion Engineering Conference, Boston, MA, Aug. 1991; reprinted in IEEE AES Systems Magazine., pp. 3-7, Nov. 1991

3. G. A. Landis, 9th Princeton/SSI Conference on Space Manufacturing, Princeton NJ, May 10-13 1989; paper published in Space Manufacturing 7 290 (AIAA, 1989). Also available as NASA Technical Memorandum TM-102127 (1989)

4. G. A. Landis, J. Propulsion and Power, Vol. 8, No. 1,251-254 (1992).

5. S. Oleson, G.A. Landis, M. Stavens and J. Bozek, paper AIAA-92-3213. 28th Joint Propulsion Conf., Nashville, TN, July 1992, .

6. N. Bloembergen et al., Lasers. Science and Technology of Directed Energy Weapons, Report of the American Physical Society Study Group, Chap 3, pp. 51-139, (1987) [see also Rev. Modern Phys. 59, No. 3, part II (1987)]

7. Boeing HAP laser. Results reported in G. Emanuel et al., Aerospace Am. 28, No. 12, 28 (1990)

8. P.A. Iles, Conf. Record 21st IEEE Photovoltaic Specialists Conf., Kissimmee, FL, May. 1990,Vol. I, 420-423.

9. L.C. Olsen et al., Conf. Record 22nd IEEE Photovoltaic Specialists Conf., Las Vegas NV, Oct. 1991,Vol. I, 419-424.

10. G.A. Landis, Conf. Record 22nd IEEE Photovoltaic Specialists Conf., Las Vegas NV, Oct. 1991, Vol. II, 1494-1502; available as NASA Contractor Report 189075 (1991).

11. D. Goodman, Review of SELENE 91 Program Results and FY 92 Program Kickoff, Dec. 10-11, 1991, NASA Marshall Spaceflight Center, p. IV-47; also Technology Workshop on Laser Beamed Power, NASA Lewis Research Center, Feb. 5 1991, p. C-15

12. APLE laser scaled to 840 nm operation. R. L. Lamb, Boeing Corporation, private communication, March 1992.

13. R. Burke, SELENE Laser Power Beaming Applications Workshop, Mar. 24, 1992, NASA Marshall Space Flight Center, AL.

14. R.K. Ahrenkiel, D.J. Dunlavy and T. Hanak, Solar Cells, Vol. 24, 339-352 (1988).

15. G.A. Landis and H. Stoddart, Conf. Record 19th IEEE Photovoltaic Specialists Conf., Kissimmee, New Orleans LA, May 1987, 761-763.

16. K. Rajkanan and J. Shewchun, Solid State Electronics Vol. 22, 193-197 (1979)

17. S.R. Wenham, F. Zhang, C.M. Chong and M.A. Green, Conf. Record. 21st IEEE Photovoltaic Specialists Conf., Kissimmee, FL, May 1990, 323-326.

18. H.F. MacMillan et al., Conf. Record. 20th IEEE Photovoltaic Specialists Conf., Las Vegas, NV, 1988, 462-468.

19. M.B. Spitzer et al., Conf. Record. 20th IEEE Photovoltaic Specialists Conf., Las Vegas, NV, 1988, 930-933.

Cell	Type	Material	Area cm ^{2}	R_{series} (Ω)[1]	I_{SC}(A)
ASEC 10 ohm-cm	planar	Si	4	.068	.47
ASEC .2 ohm-cm	"		4	.159	.16
ASEC 10 ohm-cm	planar (radiation damaged)	"	4	1.904	.29
ASEC 10 ohm-cm	concentrator		1	.182	.45
ASEC .15 ohm-cm	"	"	1	.050	.067
VARIAN	planar	GaAs	4	.093	.15
KOPIN	concentrator	"	.59	.162	.23
VS x850	"	"	.196	.100	.13
ASEC #16	planar	GaAs/Ge	4	.208	.25
BOEING A096A	planar	CIS	4	.879	.165
BOEING #6701	concentrator	GaSb	.238	.212	.09

[1] by comparison of V_{OC} vs I_{SC} against dark diode curve

Table 1 Cell Types tested under RF and Inductive FEL and CW Formats

Laser type	wavelength (nm)	correction factor
Correcting to 840 nm (GaAs cells):		
Copper Vapor Laser	511	1.64
Ar Ion Laser	514.5	1.63
Doubled YAG Laser	532	1.58
Correcting to 950 nm (Si cells)		
Copper Vapor Laser	511	1.86
Ar Ion Laser	514.5	1.85
Doubled YAG Laser	532	1.79
Correction to 1600 nm (GaSb cells)		
Copper Vapor Laser	511	3.13
Ar Ion Laser	514.5	3.11
Doubled YAG Laser	532	3.01

Table 2. Correction factor to translate efficiencies measured at test wavelength to efficiencies at longer operating wavelength, assuming equal quantum efficiency at both wavelengths.

Cells	Efficiency (%)				
	AM0	CW laser	induction FEL		
intensity (mw/cm)[2]	137	170	253	25	2.5
Silicon					
ASEC .15 ohm-cm concentrator	15.0	15.3	12.1	13.8	13.8
ASEC .2 ohm-cm	15.5	19.0	7.2	11.9	11.3
ASEC 10 ohm-cm	11.9	14.5	5.6	10.1	9.1
ASEC 10 ohm-cm(rad. damaged)	10.5	13.9	1.9	5.5	7.5
ASEC 10 ohm-cm concentrator	12.9	13.7	7.6	10.4	8.6
GaAs					
VARIAN	16.9	29.0	.15	1.5	12.0
Kopin	20.7	26.6	1.3	7.3	20.7
VS x850	19.4	21.7	2.0		
VS x850 with .5uf cap			4.5		
VS x850 with 4.4 uf cap			3.4	10.2	13.2
GaAs/Ge					
ASEC #16	17.9	26.0			
$CuInSe_2$					
Boeing A096A	8.4	5.5	.01		.5
GaSb					
Boeing #6701	5.7	1.26		.25	.26

[1] Power levels of 253, 25, and 2.5 mw/cm^2 represent the average of all individual power measurents. The exact power, measured for each cell, is used to calculate the efficiency for that cell.

Table 3 Cell Efficiency (%) with AM0, CW, and Inductive FEL Format

Cells	Efficiency (%) @ 253 mW/cm^2
Silicon	
ASEC .15 ohm-cm	22.5
ASEC 10 ohm-cm	10.4
ASEC 10 ohm-cm (rad. damaged)	3.5
GaAs	
VARIAN	.25
KOPIN	2.1
GaSb	
Boeing #6701	.81 [1]

[1] Incident power for the GaSb cell is 25.3 mW/cm

Table 4 Wavelength Corrected Efficiencies of Si, GaAs, and GaSbCells for induction FEL

Cell	Power W/cm^2	Efficiency, %	
		$I_{avg} \times V_{bias}$	$\int_0^{t_o} v(t)i(t)dt$
GaAs/Ge			
ASEC #16	16.7	3.4	5.0
GaAs			
Varian x850	16.7	1.15	.2
Varian x850 w/4.4uf cap.	16.7	24.1	30.1
Si			
ASEC .15 ohm-cm	15.0	11.1	11.8

Table 5 Comparison of cell efficiency using $I_{avg}xV_{bias}$ and the total area under the curve for P_{avg} at 530nm for the RF pulse format

Cell	V_{mp} (mV)	I_{mp} (mA)[1]	I_{dark} (mA)[2]
Induction Laser Format, 253 mW/cm^2			
Si: ASEC 10 ohm-cm	400	148	0.87
ASEC Rad. damaged	350	52	0.27
ASEC .15 ohm conc.	550	58	0.53
ASEC conc.#1 (10 Ω)	425	50	1.1
GaAs: VARIAN	650	2.0	0.028
Kopin	700	3.2	0.013
VS x850 (no cap)	725	1.33	0.030
(500 nF)	725	2.9	0.030
(4.4 uF)	650	2.45	0.012
RF Laser Format			
Si: ASEC .15 ohm conc.	600	1763	3.0
GaAs: ASEC Mantec GaAs/Ge	500	2370	0.04
VS x850 (no cap)	500	43	0.0022
(with cap)	780	596	0.064

[1] Current at maximum power point for the RF laser format is the average current over the duration of the pulse.

[2] Dark current is taken from V_{oc} - I_{sc} measurement.

Table 6: Bias voltage and current at maximum power point and dark forward current at bias voltage for Si and GaAs cells under pulsed illumination.

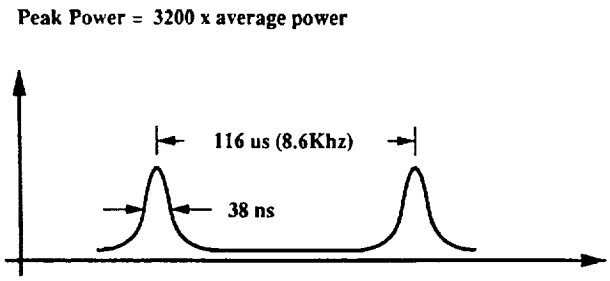

(a) Induction FEL pulse format.

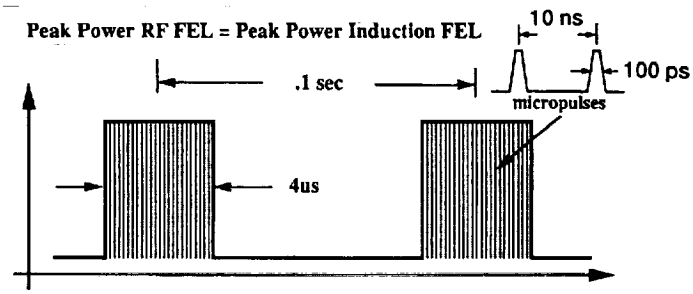

(b) RF FEL pulse format.

Figure 1.—Induction and RF FEL pulse formats.

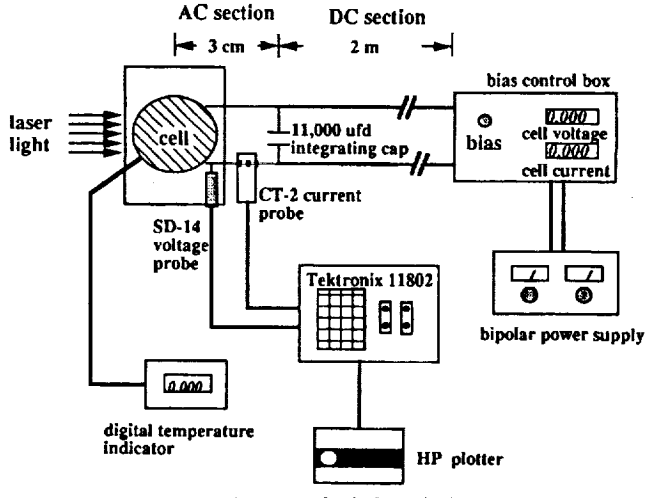

Figure 2.—Schematic of measuring circuit.

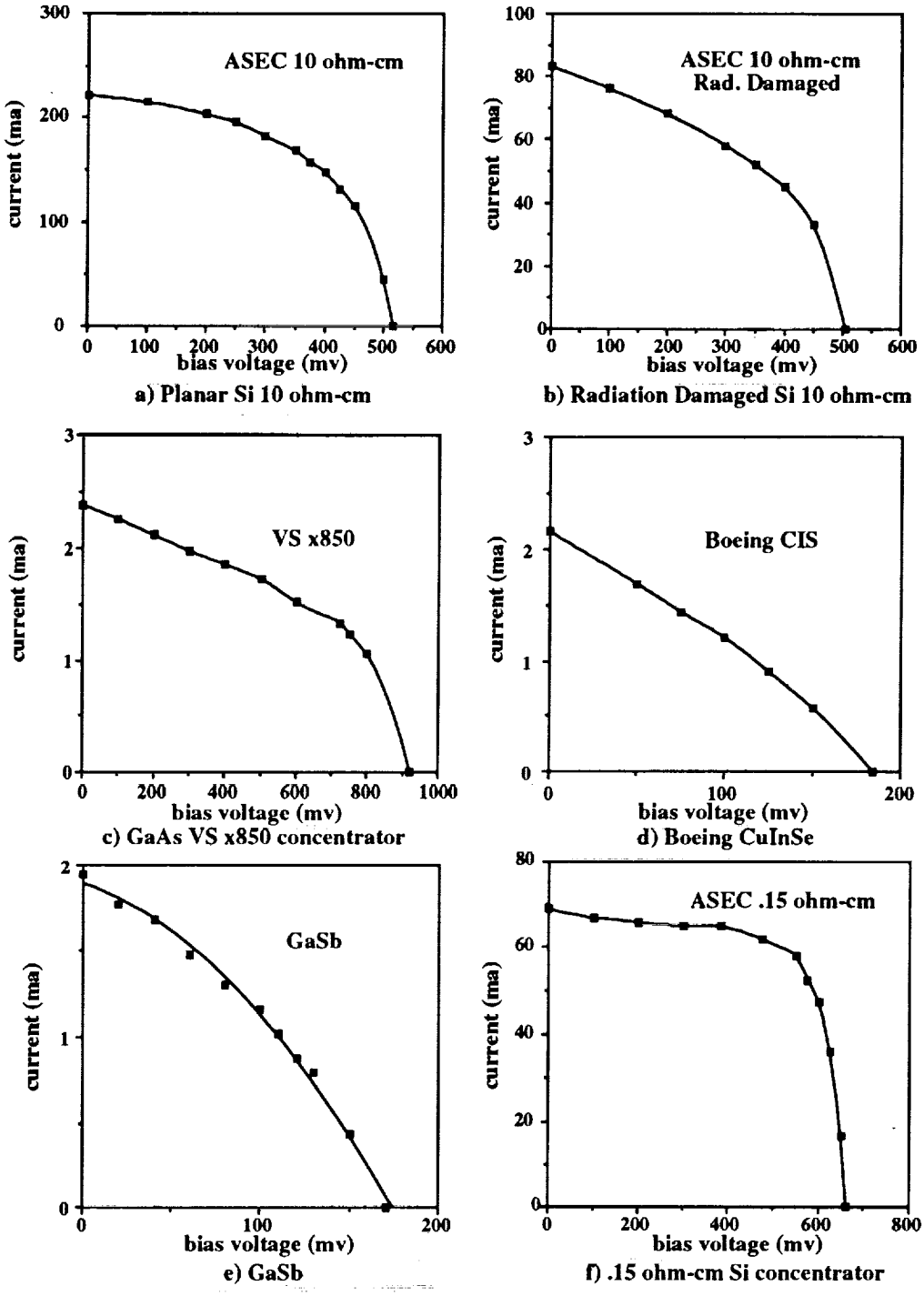

Figure 3 IV characteristics of Si, GaAs, $CuInSe_2$ and GaSb cells at 253 mW/cm^2 illumination

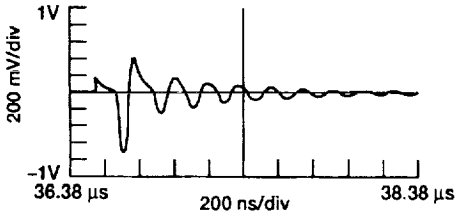

(a) Voltage response of VSx850 GaAs concentrator cell at 0V bias.

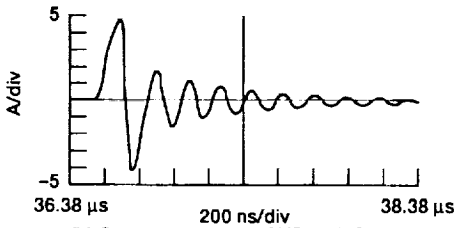

(b) Current response of VSx850 GaAs concentrator cell at 0V bias.

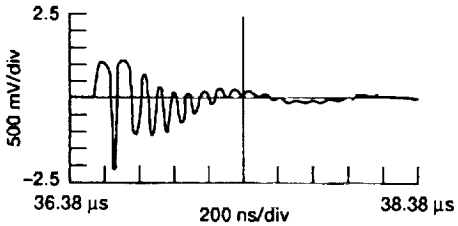

(c) Voltage response of VSx850 GaAs concentrator cell with 500 nF capacitor at 0V bias.

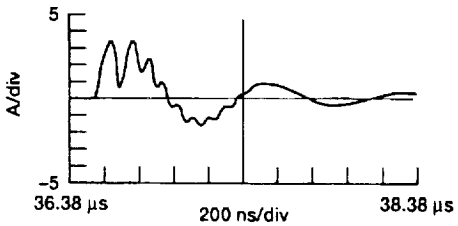

(d) Current response of VSx850 GaAs concentrator cell with 500 nF capacitor at 0V bias.

Figure 4.—Response of VSx850 GaAs concentrator cell with and without 500 nF capacitor.

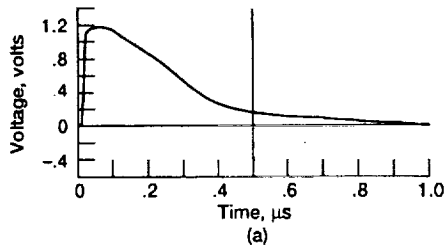

(a)

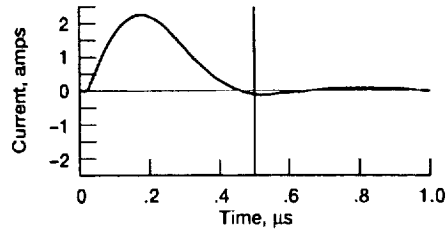

(b)

Figure 5.—Voltage and current response of GaAs planar cell to CVL (induction FEL) pulse at 0V bias.

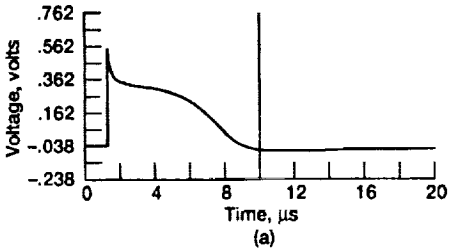

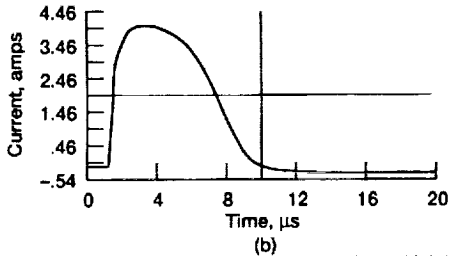

Figure 6.—Voltage and current response of ASEC 10 ohm-cm Si cell to CVL (induction FEL) pulse at 0V bias.

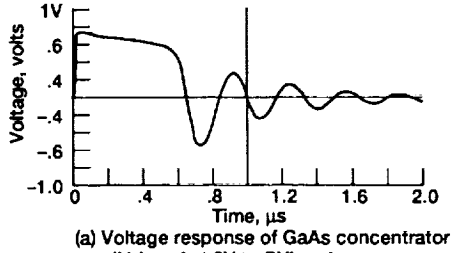

(a) Voltage response of GaAs concentrator cell biased at 0V to CVL pulse.

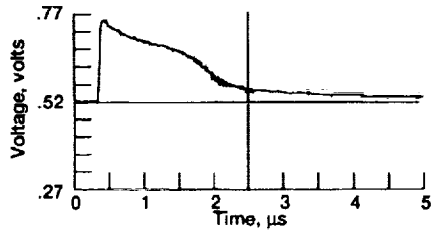

(b) Voltage response of GaAs concentrator cell biased at .52 V to CVL pulse.

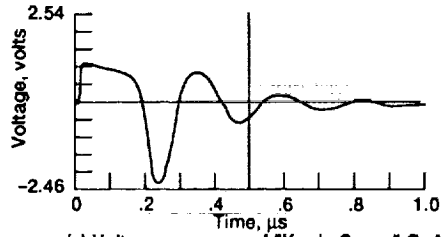

(c) Voltage response of "Kopin Super" GaAs concentrator cell at 0V bias.

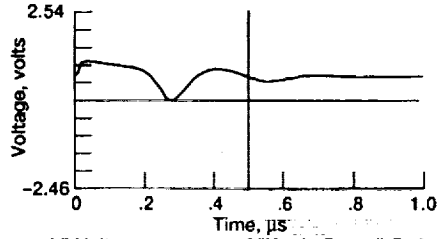

(d) Voltage response of "Kopin Super" GaAs concentrator cell at .700 V bias.

Figure 7.—Voltage response of GaAs concentrator cells showing effect of bias voltage on ringing.